

## Flexible Energy Scheduling in the Electrical, Thermal, and Gas Networks, including Energy Hubs with Renewables and Flexible Units

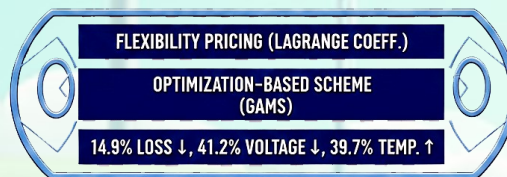
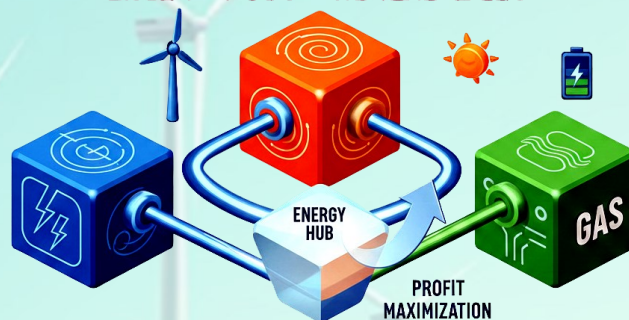
Naghi Moaddabi Pirkolachahi, Mehrdad Mallaki, Najmeh Charaghi Shirazi, Mousa Hamrahi

### Highlights

- ❖ Development of a comprehensive flexibility model for energy hubs.
- ❖ Introduction of a methodology for flexibility pricing.
- ❖ Advancement in energy network flexibility management across diverse systems.

### Graphical Abstract

## FLEXIBLE ENERGY SCHEDULING ELECTRICAL, THERMAL, & GAS NETWORKS ENERGY HUBS + RENEWABLES



KEYWORDS: FLEXIBILITY, ENERGY HUB, OPTIMIZATION

Use your device to scan  
and read the article  
online



#### Citation

M. Hamrahi, M. Mallaki, N. Moaddabi Pirkolachahi, and N. Cheraghi Shirazi, "Flexible Energy Scheduling in the Electrical, Thermal and Gas Networks including Energy Hubs with Renewables and Flexible Units," *Journal of Green Energy Research and Innovation*, vol. 2, no. 4, pp. 58-66, 2025.



<https://doi.org/10.61882/jgeri.2.4.58>





Online ISSN: 3041-9018

Journal of Green Energy Research and Innovation

Journal Homepage: [www.jgeri.araku.ac.ir](http://www.jgeri.araku.ac.ir)

# Flexible Energy Scheduling in the Electrical, Thermal, and Gas Networks, including Energy Hubs with Renewables and Flexible Units

Mousa Hamrahi, Mehrdad Mallaki<sup>\*</sup>, Naghi Moaddabi Pirkolachahi, Najmeh Charaghi Shirazi

Department of Electrical Engineering, Bu.C., Islamic Azad University, Bushehr, Iran.

## ARTICLE INFO

### Keywords:

Flexibility pricing,  
Grid-connected energy hub,  
Flexible energy management,  
Penalty function,  
Operation limit.

### Article History:

Received: 25 May 2025

Revised: 01 July 2025;

Accepted: 31 July 2025.

### Article type:

Research Article

### \* Corresponding authors

E-mail address

[mallaki@aut.ac.ir](mailto:mallaki@aut.ac.ir) (M. Mallaki)

## ABSTRACT

This paper addresses the issue of flexibility pricing for grid-connected energy hubs (EHs) under the influence of uncertain energy generation resources. An optimization-based scheme is proposed to tackle this challenge. The objective of the problem is to maximize the profitability of these resources within the flexibility market. Key constraints include the flexibility model of energy storage systems, load response mechanisms, and controllable distributed generation units. Additional restrictions involve the optimal load distribution equations across energy networks, the utilization model of EHs incorporating various active resources and loads, as well as the flexibility constraints specific to EHs. The flexibility model hinges on the active power generated by these resources. The flexibility price is determined by the Lagrange coefficients corresponding to the flexibility constraint. To compute this price, a penalty function associated with the flexibility constraint is incorporated into the objective function. The proposed framework is implemented in the GAMS software environment and tested on a 9-bus electric grid, a 4-bus gas system, and a 7-bus thermal network. Ultimately, the scheme's effectiveness in enhancing operational performance, flexibility, and economic outcomes for both energy networks and EHs is thoroughly analyzed. So that based on optimal operation of resources, storage devices, and responsive loads, total energy losses, maximum voltage drop, and temperature improvements of approximately 14.9%, 41.2%, and 39.7%, respectively, when compared to load distribution studies.

## 1. Introduction

Concerns over environmental pollution stemming from excessive fossil fuel consumption have prompted various organizations to advocate for the adoption of environmentally friendly energy sources. As a result, recent years have seen a notable rise in the integration of renewable energy sources (RES), such as wind and solar systems, into power grids. Additionally, deploying distributed generation (DG) at local consumption points diminishes reliance on centralized power plants, contributing to reduced emissions from these plants. DG technologies, including fuel cells (FC), microturbines (MT), diesel generators (DiG), and combined heat and power (CHP) systems, exhibit significantly lower pollution levels compared to traditional power plants. Moreover, energy storage systems (ESSs) and demand response programs (DRPs) play a crucial role in curbing pollution by minimizing energy losses at the consumption level. Even mobile ESSs, such as electric vehicles (EVs), contribute to reducing emissions typically associated with conventional fossil fuel-powered vehicles. However, achieving meaningful environmental benefits from these advancements relies heavily on integrating a substantial number of resources and active loads (ALs) into the power grid, particularly within distribution networks. This increased volume of data poses significant challenges for distribution system operators (DSOs), complicating network management processes. To address these complexities, smart grid principles advocate for employing resource aggregators and active loads within configurations such as virtual power plants (VPPs) and energy hubs (EHs). Managing multiple energy types simultaneously proves more effective than handling them individually, especially given the interconnected nature of diverse technologies like CHP systems. Considering the interdependence among various energy sources and the need for cohesive coordination, adopting the EH model offers an efficient framework for managing distributed energy resources and active loads comprehensively.

Numerous studies and research endeavors have focused on integrating energy hubs (EHs) into various energy networks. In reference [1], the authors explored the stochastic modeling of grid-connected EH participation in the day-ahead (DA) energy market. This study utilized EHs to coordinate RES, CHP, electric vehicle (EV) parking, battery storage, and DRP. By employing a linear approximation model, the problem in [1] was solved with optimal solutions with reduced computational time. Findings from this study demonstrated that the coordinated management of resources and ALs within the EH framework provided greater financial benefits compared to their independent operation. Additionally, the optimal scheduling of EHs significantly enhanced key performance metrics for electricity, gas, and heat networks. This improvement included reduced energy losses, as shown in power distribution studies, and smoother voltage, pressure, and temperature profiles. In study [2], EHs were employed to coordinate RES, batteries, and CHP systems, focusing on their role in the electricity, gas, and heat sectors. The electricity component of the EH participated in two energy market models: power pool and bilateral contracts. Results from [2] supported the findings of [1], confirming the capability of EHs in improving both the operational performance and economic outcomes of the integrated networks. The stochastic operational model of EHs analyzed in [3] incorporated renewable sources, a combined cooling, heating, and power (CCHP) system, various storage solutions, and DRPs. Leveraging storage significantly reduced operating costs. A comparable model was examined in [4], which extended the implementation to EHs connected to a microgrid. To ensure computational efficiency, [4] also adopted a linear approximation model, achieving an optimal solution with minimal error—approximately 2.5% for active and reactive power across scenarios [1-2,4]. The reliability of EHs under N-1 contingency events (i.e., element failure) was investigated in the study [5]. The results highlighted the capacity of optimally scheduled EH resources and ALs to maintain high reliability. In [6], a scenario-based stochastic operational analysis was conducted for residential EHs while considering RES uncertainties, EVs, and thermal energy storage (TES). This study also incorporated Monte Carlo simulations (MCS) to account for fluctuations in energy prices and active power output by distributed generation resources (RDGs). Findings revealed that EVs and TES played significant roles in reducing operational costs for EHs. Notably, formulating the operational framework for energy networks with EH integration is inherently nonlinear. Studies such as [1-2] and [4] employed linear approximation models (LAM) to simplify these problems for computational efficiency. Other research works, including [7-8], utilized non-linear heuristic evolutionary algorithms (NHEA) to determine optimal solutions. These included methods like modified teaching-learning-based optimization (MTLBO) in [7] and genetic algorithms (GA) in [8]. Robust modeling techniques have also been applied to address uncertainties by focusing on worst-case scenarios to derive optimized solutions. Robust optimization approaches typically exhibit lower computational time compared to stochastic programming while ensuring a favorable performance across other scenarios beyond the worst-case outcome. For instance, study [9] presented robust modeling strategies that ensured robust optimization outcomes were superior to traditional optimal responses in standard scenarios. Meanwhile, reference [10] introduced a bounded uncertainty robust optimization (BURO) method. This approach aligned uncertainty parameters with their upper or lower bounds as they related to their positions within the original problem formulation. In conclusion, extensive research has underscored the versatility of EHs in improving energy network performance and economic outcomes while leveraging advanced modeling techniques such as stochastic programming, linear approximations, heuristic algorithms, and robust optimization methodologies to address operational challenges efficiently.

The text highlights several research gaps, particularly in the domain of system flexibility modeling. Although substantial research has been conducted across diverse fields, notably energy hubs and other systems, the aspect of flexibility modeling remains inadequately explored. Accurately determining the status of a system's indicator requires numerical results that can only be obtained through mathematical modeling. Therefore, to assess the flexibility status of energy networks and EHs, integrating a mathematical model of the targeted flexibility indicator into the operational analysis of these networks is critical. Energy hubs offer multiple flexibility resources such as stationary and mobile ESSs, DRPs, and controllable distributed generation units. These resources are anticipated not only to provide essential flexibility services but also to generate financial gains through their participation. This dual-purpose approach presents an efficient method for involving these resources in flexibility services. However, the academic and practical discourse around this topic has been relatively minimal, leaving significant research gaps unaddressed. To address these gaps, this paper introduces a framework for tackling the flexibility pricing problem in grid-connected energy hubs under conditions of uncertain energy generation. The proposed solution employs an optimization-based approach, aiming to maximize the financial benefits of these resources within the flexibility market. The problem formulation incorporates constraints such as the flexibility models of energy storage systems, responsive loads, and controllable distributed generation. Additional constraints include optimal load distribution equations for energy networks, utilization models for EHs with integrated active resources and loads, and specific flexibility limitations of EHs. The flexibility models for these resources depend on their active power contributions to the system. To quantify flexibility pricing, the Lagrange multipliers associated with the flexibility constraints are utilized. A penalty function corresponding to these constraints is incorporated into the objective function, ensuring accurate pricing. The key contributions of this work are summarized as follows: 1) Development of a comprehensive flexibility model for energy hubs. 2) Introduction of a methodology for flexibility pricing. 3) Advancement in energy network flexibility management across diverse systems.

Section 2 outlines the problem's formulation. Section 3 details the test system. Section 4 provides the numerical results, followed by the conclusion in Section 5.

## 2. Formulation

Formulation of the problem is as Equation (1).

$$\begin{aligned} \max \quad \text{Profit} = & \sum_s \rho_s \sum_{i,t} \left( \bar{\lambda}_{i,t,s}^{ef} EF_{i,t,s}^U + \underline{\lambda}_{i,t,s}^{ef} EF_{i,t,s}^D \right) + \\ & \sum_s \rho_s \sum_{i,t} \left( \bar{\lambda}_{i,t,s}^{hf} HF_{i,t,s}^U + \underline{\lambda}_{i,t,s}^{hf} HF_{i,t,s}^D \right) \end{aligned} \quad (1)$$

Subject to Equations (2)-(48).

$$EF_{i,t,s}^U = UF_{i,t,s}^{DRPe} + UF_{i,t,s}^{EES} + UF_{i,t,s}^{CHP} \quad \forall i,t,s \tag{2}$$

$$EF_{i,t,s}^D = DF_{i,t,s}^{DRPe} + DF_{i,t,s}^{EES} + DF_{i,t,s}^{CHP} \quad \forall i,t,s \tag{3}$$

$$HF_{i,t,s}^U = UF_{i,t,s}^{DRPh} + UF_{i,t,s}^{TES} \quad \forall i,t,s \tag{4}$$

$$HF_{i,t,s}^D = DF_{i,t,s}^{DRPh} + DF_{i,t,s}^{TES} \quad \forall i,t,s \tag{5}$$

$$UF_{i,t,s}^{DRPe} - DF_{i,t,s}^{DRPe} = P_{i,t,s}^{DRP} - P_{i,t,s=1}^{DRP} \quad \forall i,t,s \tag{6}$$

$$UF_{i,t,s}^{EES} - DF_{i,t,s}^{EES} = (P_{i,t,s}^{DCH} - P_{i,t,s}^{CH}) - (P_{i,t,s=1}^{DCH} - P_{i,t,s=1}^{CH}) \quad \forall i,t,s \tag{7}$$

$$UF_{i,t,s}^{CHP} - DF_{i,t,s}^{CHP} = P_{i,t,s}^{CHP} - P_{i,t,s=1}^{CHP} \quad \forall i,t,s \tag{8}$$

$$UF_{i,t,s}^{DRPh} - DF_{i,t,s}^{DRPh} = H_{i,t,s}^{DRP} - H_{i,t,s=1}^{DRP} \quad \forall i,t,s \tag{9}$$

$$UF_{i,t,s}^{TES} - DF_{i,t,s}^{TES} = (H_{i,t,s}^{DCH} - H_{i,t,s}^{CH}) - (H_{i,t,s=1}^{DCH} - H_{i,t,s=1}^{CH}) \quad \forall i,t,s \tag{10}$$

$$UF, DF \geq 0 \quad \forall i,t,s \tag{11}$$

$$P_{ne,t,s}^S + \sum_i K_{ne,i}^E P_{i,t,s}^{EH} - \sum_l L_{ne,l}^E P_{ne,l,t,s}^L = P_{ne,t,s}^D \quad \forall ne,t,s \tag{12}$$

$$Q_{ne,t,s}^S + \sum_i K_{ne,i}^E Q_{i,t,s}^{EH} - \sum_l L_{ne,l}^E Q_{ne,l,t,s}^L = Q_{ne,t,s}^D \quad \forall ne,t,s \tag{13}$$

$$H_{nh,t,s}^S + \sum_i K_{nh,i}^H H_{i,t,s}^{EH} - \sum_l L_{nh,l}^H H_{nh,l,t,s}^L = H_{nh,t,s}^D \quad \forall nh,t,s \tag{14}$$

$$G_{ng,t,s}^S + \sum_i K_{ng,i}^G G_{i,t,s}^{EH} - \sum_l L_{ng,l}^G G_{ng,l,t,s}^L = G_{ng,t,s}^D \quad \forall ng,t,s \tag{15}$$

$$P_{ne,l,t,s}^L = g_{ne,l}^L (V_{ne,t,s})^2 - V_{ne,t,s} V_{l,t,s} \{ g_{ne,l}^L \cos(\alpha_{ne,t,s} - \alpha_{l,t,s}) + b_{ne,l}^L \sin(\alpha_{ne,t,s} - \alpha_{l,t,s}) \} \quad \forall ne,l,t,s \tag{16}$$

$$Q_{ne,l,t,s}^L = -b_{ne,l}^L (V_{ne,t,s})^2 + V_{ne,t,s} V_{l,t,s} \{ b_{ne,l}^L \cos(\alpha_{ne,t,s} - \alpha_{l,t,s}) - g_{ne,l}^L \sin(\alpha_{ne,t,s} - \alpha_{l,t,s}) \} \quad \forall ne,l,t,s \tag{17}$$

$$H_{nh,l,t,s}^L = \varpi_{nh,l} (T_{nh,t,s} - T_{l,t,s}) \quad \forall nh,l,t,s \tag{18}$$

$$G_{ng,l,t,s}^L = v_{ng,l} \text{sign}(\beta_{ng,t,s}, \beta_{l,t,s}) \sqrt{\text{sign}(\beta_{ng,t,s}, \beta_{l,t,s}) ((\beta_{ng,t,s})^2 - (\beta_{l,t,s})^2)} \quad \forall ng,l,t,s \tag{19}$$

$$V_{ne}^{\min} \leq V_{ne,t,s} \leq V_{ne}^{\max} \quad \forall ne,t,s \tag{20}$$

$$T_{nh}^{\min} \leq T_{nh,t,s} \leq T_{nh}^{\max} \quad \forall nh,t,s \tag{21}$$

$$\beta_{ng}^{\min} \leq \beta_{ng,t,s} \leq \beta_{ng}^{\max} \quad \forall ng,t,s \tag{22}$$

$$\sqrt{(P_{ne,l,t,s}^L)^2 + (Q_{ne,l,t,s}^L)^2} \leq S_{ne,l}^{L \max} \quad \forall ne,l,t,s \tag{23}$$

$$-H_{nh,l,t,s}^{L \max} \leq H_{nh,l,t,s}^L \leq H_{nh,l,t,s}^{L \max} \quad \forall nh,l,t,s \tag{24}$$

$$-G_{ng,l,t,s}^{L \max} \leq G_{ng,l,t,s}^L \leq G_{ng,l,t,s}^{L \max} \quad \forall ng,l,t,s \tag{25}$$

$$\sqrt{(P_{ne,t,s}^S)^2 + (Q_{ne,t,s}^S)^2} \leq S_{ne}^{S \max} \quad \forall ne = o,t,s \tag{26}$$

$$-H_{nh}^{S \max} \leq H_{nh,t,s}^S \leq H_{nh}^{S \max} \quad \forall nh = o,t,s \tag{27}$$

$$-G_{ng}^{S \max} \leq G_{ng,t,s}^S \leq G_{ng}^{S \max} \quad \forall ng = o,t,s \tag{28}$$

$$P_{i,t,s}^{EH} = P_{i,t,s}^{CHP} + P_{i,t,s}^{RES} + P_{i,t,s}^{DRP} + (P_{i,t,s}^{DCH} - P_{i,t,s}^{CH}) - P_{i,t,s}^D \quad \forall i,t,s \tag{29}$$

$$Q_{i,t,s}^{EH} = Q_{i,t,s}^{CHP} - Q_{i,t,s}^D \quad \forall i,t,s \tag{30}$$

$$H_{i,t,s}^{EH} = H_{i,t,s}^{CHP} + H_{i,t,s}^{DRP} + (H_{i,t,s}^{DCH} - H_{i,t,s}^{CH}) - H_{i,t,s}^D \quad \forall i,t,s \tag{31}$$

$$G_{i,t,s}^{EH} = -G_{i,t,s}^{CHP} - G_{i,t,s}^D \quad \forall i,t,s \tag{32}$$

$$H_{i,t,s}^{CHP} = P_{i,t,s}^{CHP} \frac{(1 - \eta^T - \eta^L) \eta^H}{\eta^T} \quad \forall i,t,s \tag{33}$$

$$G_{i,t,s}^{CHP} = P_{i,t,s}^{CHP} \frac{1}{\eta^T} \quad \forall i,t,s \tag{34}$$

$$\sqrt{(P_{i,t,s}^{CHP})^2 + (Q_{i,t,s}^{CHP})^2} \leq S_i^{CHP \max} \quad \forall i,t,s \tag{35}$$

$$-H_i^{CHP \max} \leq H_{i,t,s}^{CHP} \leq H_i^{CHP \max} \quad \forall i,t,s \tag{36}$$

$$-\omega_t P_{i,t,s}^D \leq P_{i,t,s}^{DRP} \leq \omega_t P_{i,t,s}^D \quad \forall i,t,s \quad (37)$$

$$\sum_i P_{i,t,s}^{DRP} = 0 \quad \forall i,s \quad (38)$$

$$-\omega_t H_{i,t,s}^D \leq H_{i,t,s}^{DRP} \leq \omega_t H_{i,t,s}^D \quad \forall i,t,s \quad (39)$$

$$\sum_i H_{i,t,s}^{DRP} = 0 \quad \forall i,s \quad (40)$$

$$0 \leq P_{i,t,s}^{CH} \leq ECR_i \quad \forall i,t,s \quad (41)$$

$$0 \leq P_{i,t,s}^{DCH} \leq EDR_i \quad \forall i,t,s \quad (42)$$

$$E_i^{\min} \leq EI_i + \sum_{h=1}^t \left( \eta_i^{CH} P_{i,h,s}^{CH} - \frac{1}{\eta_i^{DCH}} P_{i,h,s}^{DCH} \right) \leq E_i^{\max} \quad \forall i,t,s \quad (43)$$

$$0 \leq H_{i,t,s}^{CH} \leq HCR_i \quad \forall i,t,s \quad (44)$$

$$0 \leq H_{i,t,s}^{DCH} \leq HDR_i \quad \forall i,t,s \quad (45)$$

$$E_i^{\min} \leq EI_i + \sum_{h=1}^t \left( \eta_i^{CH} H_{i,h,s}^{CH} - \frac{1}{\eta_i^{DCH}} H_{i,h,s}^{DCH} \right) \leq E_i^{\max} \quad \forall i,t,s \quad (46)$$

$$-\Delta F \leq P_{i,t,s}^{EH} - P_{i,t,s=1}^{EH} \leq \Delta F : \underline{\lambda}_{i,t,s}^{ef}, \bar{\lambda}_{i,t,s}^{ef} \quad \forall i,t,s \quad (47)$$

$$-\Delta F \leq H_{i,t,s}^{EH} - H_{i,t,s=1}^{EH} \leq \Delta F : \underline{\lambda}_{i,t,s}^{hf}, \bar{\lambda}_{i,t,s}^{hf} \quad \forall i,t,s \quad (48)$$

This section focuses on the expected profit maximization of flexibility sources (FSs) deriving from offering flexibility services in energy hubs (EHs), as defined by the objective function in Equation (1) [11]. In the context of flexibility management, two operational models are examined: 1. When the real-time (RT) RES power exceeds the DA scheduled power. Here, FSs are required to reduce their power injection into the system during RT operation compared to the DA operation. This is referred to as the downward flexibility operating mode. 2. Conversely, when the RT RES power is less than the DA scheduled power, FSs operate in the inverse manner of the first mode, described as upward flexibility. As such, flexibility pricing in Equation (1) accounts for these two operational modes: downward and upward. The first term of the equation captures the revenue earned by electric FSs from providing flexibility services in the electrical domain of EHs [11]. The second term addresses the benefits gained from providing flexibility services within the thermal domain. In Equations (2) and (3), the total flexible power provided by electric FSs under upward and downward operational modes in EHs is modeled. Correspondingly, Equations (4) and (5) establish a similar representation for the thermal domain within EHs. Equations (6) through (10) detail the flexible power contributions across different components: electric DRP, EES, CHP, thermal DRP, and TES under both operational modes. To enhance flexibility from a modeling standpoint, minimizing system deviations in active (thermal) power under scenarios relative to those in a deterministic scenario (scenario 1, based on predicted uncertainties) is crucial. Within Equations (6)-(10), flexible power for FSs is computed as the difference between the active power of FSs under scenario  $s$  and the baseline deterministic scenario. A positive deviation value represents flexible power under the upward operating mode; otherwise, it corresponds to downward operation. Notably, these power values always remain positive as defined in Equation (11). The network Equations for this model are detailed within Equations (12)-(28). Equations (12)-(19) represent the power distribution model across electrical, thermal, and gas networks [12-14]. Specifically, Equations (12) and (13) handle active and reactive power balances across electrical network buses, respectively. Equation (14) ensures thermal power balance at thermal network nodes, while Equation (15) addresses gas power balance within gas network nodes. Similarly, Equations (16)-(19) calculate active and reactive power flow through electric lines, thermal power flow within heat pipes, and gas power flow passing through gas pipelines. Operational restrictions across networks are presented in Equations (20)-(28): Voltage, temperature, and pressure range limitations are incorporated in Equations (20), (21), and (22), respectively. Apparent power limits for electric lines, along with thermal and gas flow limits for pipelines, are included in Equations (23)-(25). Analogous limitations for substations servicing electrical, thermal, and gas networks are outlined in Equations (26)-(28) [15-17].

The performance formulation of EHs is detailed across Equations (29)-(48). Equations (29)-(32) specifically model the balancing of active, reactive, thermal, and gas power within EHs. The operational modeling of CHP systems is described in Equations (33)-(36). Here, Equations (33) and (34) determine the thermal and gas power generated by the CHP, derived from its active power output. Meanwhile, the limitations of CHP's output capacity for electrical and thermal energy are addressed in Equations (35) and (36), respectively [10-11]. The electrical DRP framework appears in Equations (37)-(38) [18]. Equation (37) incorporates the active power control range into the program. Within this program, it is assumed that the energy demands of consumers must be fully met within the operational time horizon, and this requirement is enforced by Equation (38). Similarly, the thermal DRP performance follows a comparable structure to its electrical counterpart, aligning with Equations (39)-(40) while sharing Equations (37),(38). The main distinction lies in replacing variable  $P$  with variable  $H$  to represent thermal power. In this study, the gas network is treated solely as a source for CHP-generated electricity or heat; hence, no DRP model is considered for gas usage. The functional model for EES is laid out in Equations (41)-(43) [19]. Notably, an aggregation model for EVs shares similarities with these Equations but incorporates time ( $t$ ) and scenario ( $s$ ) indices to account for dynamic EV connectivity to EHs. Parameters such as  $ECR$ ,  $EDR$ ,  $EI$ ,  $Emin$ , and  $Emax$  adjust based on these indices. At any given moment or scenario,  $ECR$  and  $EDR$  represent the cumulative charging and discharging rates of EVs connected to the EH.

Hourly  $EI$  reflects the initial energy contributions of newly connected EVs during that time.  $Emin$  corresponds to the aggregated

minimum energy levels of all connected EVs, while  $E_{max}$  signifies the total future trip energy requirements of these vehicles. In the EV aggregation model's Equations, the equality operator replaces the less-than-or-equal-to operator from Equation (43) [1,10]. The formulation for TES operation is presented in Equations (44)-(46), mimicking the structure of Equations (41)-(43) but substituting variable  $P$  with  $H$  to reflect thermal energy considerations. Finally, EH flexibility constraints for the electrical and thermal sectors are expressed through Equations (47) and (48). From a mathematical modeling perspective, enhancing flexibility involves minimizing deviations in active or thermal power outputs in a given scenario when compared to those in the baseline deterministic model (scenario  $s = 1$ ) [20]. Equations (47) and (48) impose an upper limit of  $\Delta F$  on these deviations, where  $\Delta F$  represents flexibility tolerance. Setting  $\Delta F$  to zero implies complete (100%) flexibility. The dual variables associated with these constraints correspond to flexibility prices [11]. Flexibility prices are derived by incorporating the penalty functions of Equations (47) and (48) into the objective function as detailed in Equation (49). This enables simultaneous calculation of both primary and dual variables by the solver. For a constraint of the form  $a \leq b$ , the corresponding penalty function is defined as  $\lambda \cdot \max(0, a - b)$ , where  $\lambda$  represents the dual variable of the constraint.

$$\begin{aligned} \max \text{ Profit} = & \sum_s \rho_s \sum_{i,t} \left( \bar{\lambda}_{i,t,s}^{ef} EF_{i,t,s}^U + \underline{\lambda}_{i,t,s}^{ef} EF_{i,t,s}^D \right) + \\ & \sum_s \rho_s \sum_{i,t} \left( \bar{\lambda}_{i,t,s}^{hf} HF_{i,t,s}^U + \underline{\lambda}_{i,t,s}^{hf} HF_{i,t,s}^D \right) + \\ & \sum_{i,t,s} \left( \bar{\lambda}_{i,t,s}^{ef} \max(0, P_{i,t,s}^{EH} - P_{i,t,s=1}^{EH} - \Delta F) + \underline{\lambda}_{i,t,s}^{ef} \max(0, -\Delta F - P_{i,t,s}^{EH} + P_{i,t,s=1}^{EH}) \right) + \\ & \sum_{i,t,s} \left( \bar{\lambda}_{i,t,s}^{hf} \max(0, H_{i,t,s}^{EH} - H_{i,t,s=1}^{EH} - \Delta F) + \underline{\lambda}_{i,t,s}^{hf} \max(0, -\Delta F - H_{i,t,s}^{EH} + H_{i,t,s=1}^{EH}) \right) \end{aligned} \tag{49}$$

### 3. Test system

The proposed scheme has been implemented on three types of ring networks: a 9-bus electric network, a 4-bus gas network, and a 7-bus thermal network, as illustrated in Figure 1. Detailed data for these networks can be found in [1]. The hourly load for each network is determined as the product of the peak load and the daily load factor curve, also provided in [1]. The system includes 7 EHs, whose specific locations across the different networks are depicted in Figure 1. The peak loads of these EHs, along with their components, are outlined in [1]. Two RESs are incorporated into the scheme: wind turbines (WT) and photovoltaic (PV) systems. Each has a maximum capacity of 0.25 MW, and their hourly power output is calculated by multiplying their respective capacities by a daily power generation rate curve, as documented in [1]. The scheme also utilizes two types of EES: batteries and EV aggregations. The battery specifications include a storage capacity ranging from 0.2 MWh to 1.5 MWh, with an initial energy level of 0.2 MWh. It features charging and discharging rates of 0.8 MW and an efficiency of 90% for both operations. Additionally, the system assumes the presence of 60 EVs within the EHs equipped with EV parking facilities. The number of EVs fluctuates hourly based on the product of total EVs and a daily penetration rate curve, as described in [1,11]. Key characteristics of individual EVs, including charging and discharging rates, efficiency, and energy consumption details, are also reported in [11]. Within the EHs, consumer participation in the proposed DRP is set at 40%. Furthermore, CHP units are integrated in EHs 4, 6, and 7. These units have a maximum apparent power of 1 MVA and provide up to 1 MW of thermal power. They operate with turbine efficiency at 40%, loss efficiency at 9%, and thermal efficiency at 40%. For TES within these EHs, the characteristics are similar to those of the battery storage system, except for a slightly lower charging and discharging efficiency of 80%. To enhance operational flexibility, the flexibility tolerance ( $\Delta F$ ) is specified as 0.05 per unit in this scheme, ensuring the desired level of adaptability for energy hubs.

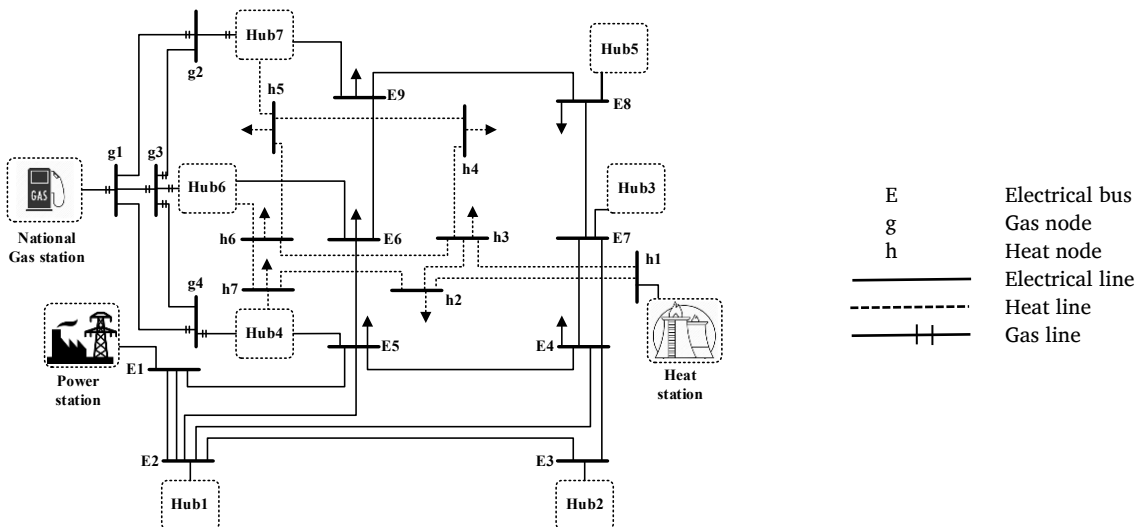


Figure 1. Test system [1].

4. Numerical results

The problem was solved by IPOPT in GAMS software [21]. Table 1 illustrates the variations in the expected value of flexibility power and the average flexibility incentive price (FIP) in the electrical and thermal sectors under ascending and descending modes, corresponding to changes in ΔF. The analysis reveals that as ΔF increases, the flexibility power diminishes. This increase in ΔF, as described by Equations (47) and (48), indicates a reduced emphasis on the flexibility of EHs within electrical and thermal networks. Consequently, a higher ΔF aligns the operations of storage generators, resources, and responsive loads more toward minimizing network operation costs, thereby leading to less contribution toward enhancing EH flexibility. As a result, flexibility power declines with rising ΔF. For instance, at elevated ΔF values, where Equations (47) and (48) are effectively disregarded, minimizing operational costs becomes significantly more critical than improving system flexibility. Under such circumstances, DRPs will typically switch to charging during periods of low demand or cheap energy prices and discharge during high load or expensive energy periods, remaining inactive at other times. On the other hand, at low ΔF values, such as when ΔF equals zero, the DRP remains active throughout, either drawing power from the grid or supplying it back. Additionally, as indicated in Table 1, an increase in ΔF also leads to a reduction in the FIP for both electrical and thermal sectors across ascending and descending modes. This outcome is directly tied to a decline in the flexibility capacity within these sectors and operating conditions. Finally, Figure 2 presents the trend of flexibility service providers' (FSSs) profits within the flexibility market as ΔF varies. The graph demonstrates that rising ΔF results in decreased FSSs' profits due to reductions in both FIP and flexibility power, as outlined in Table 1. This reflects the diminishing role of flexibility under these conditions.

Table 2 presents operational indicators for two study scenarios within electric, gas, and heat networks. Case I involves analyzing load distribution across these networks, while Case II focuses on the proposed design for varying levels of ΔF. The table includes data on energy losses, maximum voltage drops (or pressure/temperature decreases), and maximum overvoltage (or pressure/temperature increases). In Case I, all indicator values for the gas network are zero due to the absence of consumers. However, these indicators show significant levels within the electric and heat networks. Total energy losses are quantified at 7.42 MWh. The maximum voltage drop and temperature drop reach 0.114 and 0.121 per unit, respectively, both exceeding the allowable limit of 0.1 per unit (based on the range of 0.9 to 1). No overvoltage or temperature increase is observed in this scenario. In Case II, for ΔF = 0 (representing 100% flexibility), energy losses are notably reduced in the electric and heat networks by approximately 33.1% and 31.5%, respectively, compared to Case I. Conversely, the gas network experiences an energy loss increase of 1.32 MWh relative to Case I. Overall, total network energy losses decrease by about 14.9% in this scenario compared to Case I. Regarding operational improvements in Case II, the maximum pressure drop rises slightly to 0.042 per unit, while maximum overvoltage and temperature increases reach 0.025 and 0.031 per unit, respectively. However, there is a significant reduction in maximum voltage drop and temperature drop by 41.2% and 39.7%, respectively, compared to Case I. Moreover, all voltage, temperature, and pressure values remain within permissible limits (0.9 to 1.1 per unit) under this scenario. It is important to note that as ΔF increases, the performance improvement of these indicators becomes more pronounced compared to Case I. This is because decreasing the emphasis on flexibility (i.e., increasing ΔF) allows EHs to prioritize optimizing network operations, as reflected in the data presented in Table 2.

Table 1. Value of flexibility power and FIP in ΔF.

ΔF (p.u.)	0	0.05	0.20
$\sum_{i,t,s} \rho_s EF_{i,t,s}^U$ (p.u.)	14.09	11.97	8.34
$\sum_{i,t,s} \rho_s EF_{i,t,s}^D$ (p.u.)	4.5	3.99	2.78
$\sum_{i,t,s} \rho_s HF_{i,t,s}^U$ (p.u.)	12.43	10.56	7.36
$\sum_{i,t,s} \rho_s HF_{i,t,s}^D$ (p.u.)	4.15	3.52	2.46
$\frac{1}{24 \times 7} \sum_{i,t,s} \rho_s \bar{\lambda}_{i,t,s}^{ef}$ (\$/MWh)	5.99	4.37	2.34
$\frac{1}{24 \times 7} \sum_{i,t,s} \rho_s \underline{\lambda}_{i,t,s}^{ef}$ (\$/MWh)	2.47	1.80	0.92
$\frac{1}{24 \times 7} \sum_{i,t,s} \rho_s \bar{\lambda}_{i,t,s}^{hf}$ (\$/MWh)	5.57	4.06	2.08
$\frac{1}{24 \times 7} \sum_{i,t,s} \rho_s \underline{\lambda}_{i,t,s}^{hf}$ (\$/MWh)	2.29	1.66	0.85

Table 2. Operation indices value in ΔF.

Parameter	Energy loss (MWh) in electrical, heat, and gas networks				Maximum drop (p.u.) of			Maximum over (p.u.) -		
	Electrical	Heat	Gas	Total	Voltage	Temperature	Pressure	Voltage	Temperature	Pressure
Case I	5.21	2.20	0	7.42	0.114	0.121	0	0	0	0
Case II for ΔF = 0	3.48	1.51	1.32	6.32	0.067	0.073	0.042	0.025	0.031	0
ΔF = 0.05	3.42	1.46	1.31	6.20	0.067	0.073	0.042	0.027	0.033	0
ΔF = 0.10	3.35	1.41	1.31	6.08	0.066	0.072	0.042	0.028	0.034	0

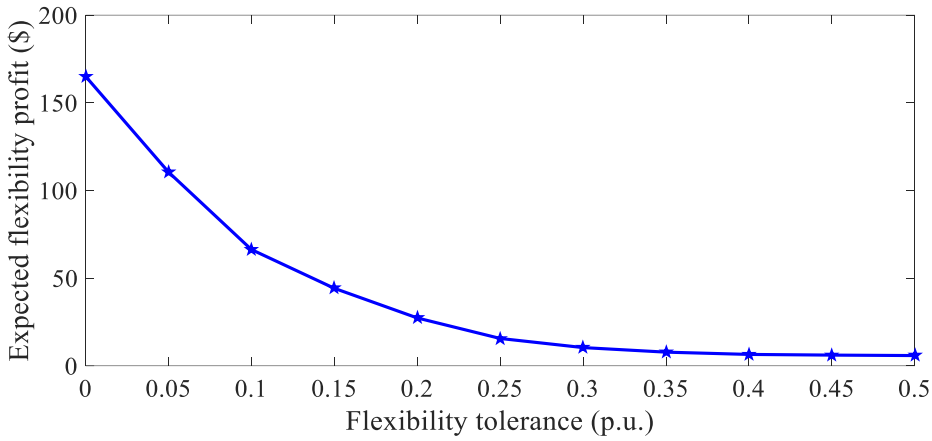


Figure 2. Flexibility profit curve in ΔF.

5. Conclusion

This paper delves into the pricing mechanisms for flexibility within EHs, focusing on electric, gas, and heat networks. The proposed framework aims to optimize the profitability of flexible resources housed within EHs by considering their specific flexibility models. Key constraints include the optimal power flow equations for the energy networks and the operational models of these hubs. From the analyzed data, several insights emerged: 1) A decrease in flexibility tolerance boosts the power of flexible resources, subsequently raising flexibility prices. 2) This adjustment significantly enhances the profits of flexible resources participating in the flexibility market within EHs. 3) Optimal operation of resources, storage devices, and responsive loads in this framework leads to improved network performance, with total energy losses, maximum voltage drop, and temperature improvements when compared to load distribution studies. 4) Maximum pressure drop and overvoltage, as well as temperature and pressure readings, remain within acceptable limits but show an upward trend compared to load distribution studies. 5) Increasing the emphasis on flexibility or reducing flexibility tolerance can elevate network operating costs. 6) The proposed model successfully achieves full flexibility conditions, effectively tolerating zero flexibility. 7) Enhanced flexibility levels correlate with increases in network energy losses, voltage drop, and temperature drop.

EHs are located in consumption areas. Therefore, if a fault occurs in the network, the EH can supply part of the energy consumed by the consumers. Therefore, the EH can be effective in improving the reliability and resilience of the network. This issue is considered as future work in the proposed design.

List of symbols

Variables (in p.u.)

- Flexibility power of electrical DRP, EES, CHP in downward mode
- Flexibility power of thermal DRP, TES in downward mode
- Hub flexibility power in upward and downward modes in the electrical section
- Gas and heat power of EH
- Gas and heat power of the line
- Gas and heat power of the substation
- Thermal power of TES for charging and discharging modes
- Hub flexibility power in upward and downward modes in the heat section
- Hub active and reactive power
- Active power of EES for charging and discharging modes
- Active, reactive, heat, and gas power of CHP
- Active and heat power of DRP
- Active and reactive power of the line
- Active and reactive power of the substation
- Temperature
- Flexibility power of electrical DRP, EES, CHP in upward mode
- Flexibility power of thermal DRP, TES in upward mode
- Range and angle of voltage
- Pressure
- FIP in the electrical section
- FIP in thermal section

- $D_{DRPe}^{FORPe}, D_{EES}^{EES}, D_{CHP}^{CHP}$
- $D_{DRPth}^{FORPth}, D_{TES}^{TES}$
- $EP^e, EF^e$
- $G^{EH}, H^{EH}$
- $G^l, H^l$
- $G^s, H^s$
- $H^{CH}, H^{DCH}$
- $HP^e, HP^t$
- $P^{EH}, Q^{EH}$
- $P^{CH}, P^{DCH}$
- $P^{CHP}, Q^{CHP}, H^{CHP}, G^{CHP}$
- $P^{DRP}, H^{DRP}$
- $P^l, Q^l$
- $P^s, Q^s$
- $T$
- $UF_{DRPe}^{DRPe}, UF_{EES}^{EES}, UF_{CHP}^{CHP}$
- $UF_{DRPth}^{DRPth}, UF_{TES}^{TES}$
- $V, \alpha$
- $\beta$
- $\lambda^{ef}, \bar{\lambda}^{ef}$
- $\underline{\lambda}^{ef}, \bar{\lambda}^{ef}$

Parameters (in p.u.)

- Charge and discharge rates in EES
- Initial energy in EES
- Min and Max of stored energy in EES
- Charge and discharge rates in TES
- Gas and heat load
- Max capacity in electrical, heat, and gas lines
- Max capacity in electrical, heat, and gas stations
- Max of heat and apparent power of CHP
- Active and reactive load
- Min and max values of temperature

- $ECR, EDR$
- $EI$
- $E^{min}, E^{max}$
- $HCR, HDR$
- $G^l, H^l$
- $G^{lmax}, H^{lmax}, S^{lmax}$
- $G^{smax}, H^{smax}, S^{smax}$
- $H^{CHPmax}, S^{CHPmax}$
- $P^l, Q^l$
- $T^{min}, T^{max}$

Min and max values of the voltage amplitude  
 Min and max value of pressure  
 Efficiency of EES in charge and discharge modes  
 Efficiency of turbine, loss, and heat in CHP  
 Scenario probability  
 Heat and gas constant for the pipeline  
 Consumers' contribution rate in DRP  
 Flexibility tolerance

$V^{min}, V^{max}$   
 $\beta^{min}, \beta^{max}$   
 $\eta^{CH}, \eta^{DCH}$   
 $\eta^T, \eta^L, \eta^{HT}$   
 $\rho$   
 $\sigma, \omega$   
 $\Delta F$

### Indices

Bus, heat node, and gas node  
 EH  
 Bus or node  
 Scenario  
 Hour

$ne, nh, ng$   
 $i$   
 $l$   
 $s$   
 $t$

### References

- [1] A. Dini, S. Pirouzi, M. Norouzi, and M. Lehtonen, "Grid-Connected Energy Hubs in the Coordinated Multi-Energy Management Based on Day-Ahead Market Framework," *Energy*, vol. 188, 116055, 2019.
- [2] K. Afrashi, B. Bahmani-Firoouzi, and M. Nafar, "Multicarrier Energy System Management as Mixed Integer Linear Programming," *Iranian Journal of Science and Technology, Transactions of Electrical Engineering*, vol. 45, no. 2, pp. 619–631, 2020.
- [3] A. Heidari, S. Mortazavi, and R. Bansal, "Stochastic Effects of Ice Storage on Improvement of an Energy Hub Optimal Operation Including Demand Response and Renewable Energies," *Applied Energy*, vol. 261, 114393, 2020.
- [4] M. Jalili, M. Sedighzadeh, and A. S. Fini, "Stochastic Optimal Operation of a Microgrid Based on Energy Hub Including a Solar-Powered Compressed Air Energy Storage System and an Ice Storage Conditioner," *Journal of Energy Storage*, vol. 33, 102089, 2021.
- [5] J. Faraji, H. Hashemi-Dezaki, and A. Ketabi, "Stochastic Operation and Scheduling of Energy Hub Considering Renewable Energy Sources' Uncertainty and N-1 Contingency," *Sustainable Cities and Society*, vol. 65, 102578, 2021.
- [6] P. Emrani-Rahaghi, and H. Hashemi-Dezaki, "Optimal Scenario-Based Operation and Scheduling of Residential Energy Hubs Including Plug-In Hybrid Electric Vehicle and Heat Storage System Considering the Uncertainties of Electricity Price and Renewable Distributed Generations," *Journal of Energy Storage*, vol. 33, 102038, 2021.
- [7] A. Shabanpour-Haghighi, and A. R. Seifi, "Multi-Objective Operation Management of a Multi-Carrier Energy System," *Energy*, vol. 88, pp. 430–442, 2015.
- [8] M. Moeini-Aghtaie, A. Abbaspour, M. Fotuhi-Firuzabad, and E. Hajipour, "A Decomposed Solution to Multiple-Energy Carriers Optimal Power Flow," *IEEE Transactions on Power Systems*, vol. 29, no. 2, pp. 707–716, 2014.
- [9] A. Dolatabadi, M. Jadidbonab, and B. Mohammadi-ivatloo, "Short-Term Scheduling Strategy for Wind-Based Energy Hub: A Hybrid Stochastic/IGDT Approach," *IEEE Transactions on Sustainable Energy*, vol. 10, no. 1, pp. 438–448, 2019.
- [10] H. Zafarani, S. A. Taher, and M. Shahidehpour, "Robust Operation of a Multicarrier Energy System Considering EVs and CHP Units," *Energy*, vol. 192, 116703, 2020.
- [11] M. Hamrahi, M. Mallaki, N. M. Pirkolachahi, and N. C. Shirazi, "Flexibility Pricing of Grid-Connected Energy Hubs in the Presence of Uncertain Energy Resources," *International Journal of Energy Research*, vol. 2023, pp. 1–21, 2023.
- [12] K. Afrashi, B. Bahmani-Firoouzi, and M. Nafar, "IGDT-Based Robust Optimization for Multicarrier Energy System Management," *Iranian Journal of Science and Technology, Transactions of Electrical Engineering*, vol. 45, no. 1, pp. 155–169, 2020.
- [13] M. Alipour, K. Zare, and M. Abapour, "MINLP Probabilistic Scheduling Model for Demand Response Programs Integrated Energy Hubs," *IEEE Transactions on Industrial Informatics*, vol. 14, no. 1, pp. 79–88, 2018.
- [14] M. Jadidbonab, A. Dolatabadi, B. Mohammadi-ivatloo, M. Abapour, and S. Asadi, "Risk-constrained Energy Management of PV Integrated Smart Energy Hub in the Presence of Demand Response Program and Compressed Air Energy Storage," *IET Renewable Power Generation*, vol. 13, no. 6, pp. 998–1008, 2019.
- [15] J. Liu, A. Wang, Y. Qu, and W. Wang, "Coordinated Operation of Multi-Integrated Energy System Based on Linear Weighted Sum and Grasshopper Optimization Algorithm," *IEEE Access*, vol. 6, pp. 42186–42195, 2018.
- [16] Y. Zhang, X. Wang, J. He, Y. Xu, and W. Pei, "Optimization of Distributed Integrated Multi-Energy System Considering Industrial Process Based on Energy Hub," *Journal of Modern Power Systems and Clean Energy*, vol. 8, no. 5, pp. 863–873, 2020.
- [17] D. Xu, Q. Wu, et al., "Distributed Multi-Energy Operation of Coupled Electricity, Heating, and Natural Gas Networks," *IEEE Transactions on Sustainable Energy*, vol. 11, no. 4, pp. 2457–2469, 2020.
- [18] H. Hamidpour, J. Aghaei, S. Dehghan, S. Pirouzi, and T. Niknam, "Integrated Resource Expansion Planning of Wind Integrated Power Systems Considering Demand Response Programmes," *IET Renewable Power Generation*, vol. 13, no. 4, pp. 519–529, 2019.
- [19] R. Homayoun, B. Bahmani-Firoouzi, and T. Niknam, "Multi-objective Operation of Distributed Generations and Thermal Blocks in Microgrids Based on Energy Management System," *IET Generation, Transmission & Distribution*, vol. 15, no. 9, pp. 1451–1462, 2021.
- [20] A. Jamali, J. Aghaei, et al., "Self-Scheduling Approach to Coordinating Wind Power Producers with Energy Storage and Demand Response," *IEEE Transactions on Sustainable Energy*, vol. 11, no. 3, pp. 1210–1219, 2020.
- [21] Generalized Algebraic Modeling Systems (GAMS).

## Declaration of competing interest

The authors declare that they have no known competing financial interests or personal relationships that could have appeared to influence the work reported in this paper. The ethical issues, including plagiarism, informed consent, misconduct, data fabrication and/or falsification, double publication and/or submission, redundancy, have been completely observed by the authors.

## Bibliography



**Mousa Hamrahi** was born in Bushehr, Iran in 1984. He received the B.Sc. (2011), M.Sc. (2017) and Ph.D. (2025) degrees from Islamic Azad University Science and Research branch, Bushehr, Iran, respectively, all in Electrical Engineering. His research interests include Smart Grids, Electricity Markets, Power System Dynamics and Renewable Energy Integration.

**Email:** [Mousa.hamrahi@yahoo.com](mailto:Mousa.hamrahi@yahoo.com)

**ORCID:** [0009-0001-5362-9457](https://orcid.org/0009-0001-5362-9457)

**Contribution Statement:** Formal analysis, Funding acquisition, Investigation, Methodology, Project administration, Resources, Software, Visualization, Roles/Writing-original draft, Writing-review & editing.



**Mehrdad Mallaki** was born in Bushehr, Iran in 1981. He received the B.Sc. (2004), M.Sc. (2006) and Ph.D. (2020) degrees from IUST, KNTU and AUT, respectively, all in Electrical Engineering. From 2007, he joined Islamic Azad University, Bushehr, Iran, where he is now working as Assistant Professor in electrical engineering department. His research interests include Smart Grids, Electricity Markets, Power System Dynamics and Renewable Energy Integration.

**Email:** [mallaki@aut.ac.ir](mailto:mallaki@aut.ac.ir)

**ORCID:** [0000-0002-2878-9328](https://orcid.org/0000-0002-2878-9328)

**Contribution Statement:** Investigation, Methodology, Project administration, Resources, Software, Supervision, Validation.



**Naghi Moaddabi Pirkolachahi** was born in Rasht, Iran, in 1984. He received the B.Sc. and M.Sc. degrees in Electrical Engineering from the Amirkabir University of Technology (Tehran Polytechnic), Tehran, Iran, in 2006 and 2008, respectively, and the Ph.D. degree in Electrical Engineering from the same university in 2014. He joined Islamic Azad University, Bushehr, Iran, as an Assistant Professor in 2015. His research interests include power system protection, transient stability, smart grids, and renewable energies.

**Email:** [nima.moaddabi@gmail.com](mailto:nima.moaddabi@gmail.com)

**ORCID:** [0000-0002-4226-3322](https://orcid.org/0000-0002-4226-3322)

**Contribution Statement:** Conceptualization, Data curation, Formal analysis, Funding acquisition, Investigation, Methodology, Project administration, Resources, Software.



**Najmeh Charaghi Shirazi** was born in Shiraz, Iran in 1982. She received the B.Sc. and M.Sc. degrees from Islamic Azad University of Bushehr, Iran, in 2005 and 2009, respectively, and the Ph.D. degree from the Islamic Azad University Science and Research branch, Tehran, Iran, in 2018, all in Electrical Engineering. From 2019, she joined Islamic Azad University, Bushehr, Iran, as an Assistant Professor. Her research interests include RFIC, circuit design, energy harvesting, and converters.

**Email:** [Nch\\_shirazi@yahoo.com](mailto:Nch_shirazi@yahoo.com)

**ORCID:** [0000-0001-6113-537X](https://orcid.org/0000-0001-6113-537X)

**Contribution Statement:** Validation, Visualization, Roles/Writing-original draft, Writing-review & editing.